TEMPORAL CHARACTERISTICS OF A SASE FEL[*]

Y. Li[#], Z. Huang, J. Lewellen, S. V. Milton, V. Sajaev, K.-J. Kim, ANL, Argonne, IL 60439, USA

Abstract

We have performed a single-shot, time-resolved measurement of the output field of a SASE FEL using the frequency-resolved optical gating (FROG) technique. The measurement reveals the phase and the amplitude of the SASE output as functions of time and frequency, hence enables us to perform a full characterization of the SASE FEL output. We examined both the single-shot field evolution as well as the statistics over multiple shots on the phase and intensity evolution.

INTRODUCTION

In a SASE FEL, a favorable instability occurs due to the interaction of an electron beam and the electromagnetic wave it produces as the beam propagates down an undulator. Provided the interaction is strong enough, the radiation power grows exponentially with the undulator distance until it reaches saturation [1,2]. Due to the mirrorless operation, such single-pass, SASE FELs are proposed for the next generation of high-brightness, coherent X-ray sources [3,4]. Recent experiments have demonstrated saturation of such SASE FELs [5-7] and their capability of achieving shorter and tunable wavelengths by direct amplification [6] as well as by harmonic generation [7,8].

We report the first single-shot time-resolved characterization of SASE pulses using the frequency-resolved optical gating (FROG) technique [9]. The measurement revealed the phase and intensity evolution of the FEL and their statistics over multiple shots. In this paper we will concentrate on the phase evolution [10].

EXPERIMENT

The measurements were conducted at the low-energy undulator test line at the Advanced Photon Source [5,10]. Table 1 is a summary of the main parameters for the two experiments. Briefly, a high-brightness electron bunch generated from an rf photocathode gun is compressed through a magnetic chicane, accelerated to 217 MeV in energy, and sent into an undulator line. A full diagnostic system for the FEL output and the electron bunch are installed at each undulator, enabling us to verify the gain of the FEL [5,11]. A mirror at each station can direct the SASE light toward diagnostics located outside of the tunnel, where the FROG device resides.

Table 1: Experimental Parameters

Experiment	A	B
Peak current	850 A	530 A
Effective bunch length (σ_z)	0.5 ps	0.13 ps
Energy chirp (σ_δ/σ_z)	28 m^{-1}	65 m^{-1}
rms normalized emittance	9 π μm	6 π μm
Undulator period (λ_u)	3.3 cm	
Undulator length (each)	2.4 m	
Undulator parameter (K)	3.1	
Beam energy (γmc^2)	217 MeV	
Nominal wavelength (λ)	530 nm	
Repetition rate	6 Hz	
Gain length (L_G)	0.68 m	0.87 m
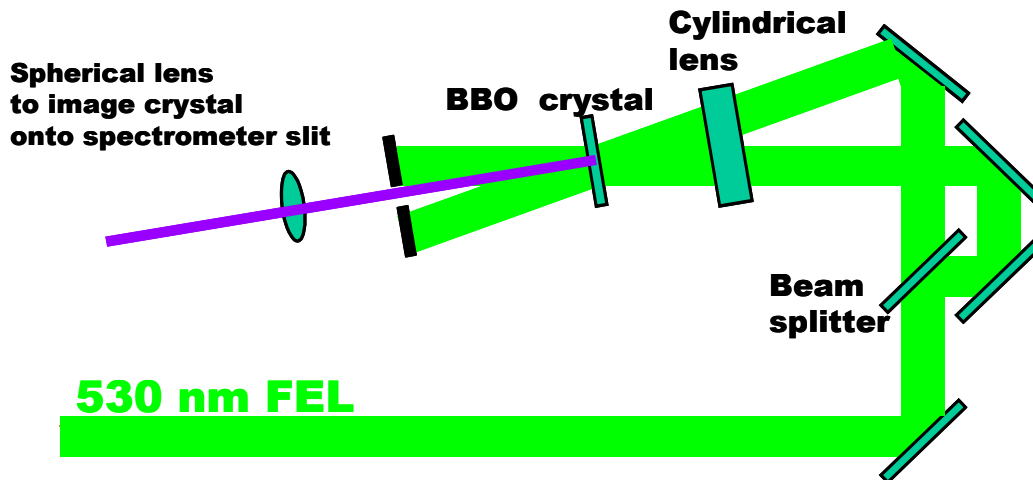
Figure 1: Setup of the second harmonic frequency-resolved optical gating device.

Negative energy chirp of the electron bunch σ_δ/σ_z in data set A is determined by energy spread on a spectrometer using a modified linac zero-phasing technique. Here σ_δ is the relative correlated energy spread, and σ_z is the rms bunch length. Exponential gain was verified by measuring the FEL output as a function of the distance along the undulators.

A single-shot FROG device using the second harmonic gating geometry [9] records single-shot spectrograms (see Fig. 1 for the device setup). In this configuration, the signal is $I_{FROG}(\omega,\tau) \propto \left| \int_{-\infty}^{\infty} E(t-\tau)E(t)\exp(-i\omega t)dt \right|^2$, where E is the field of the optical pulse and contains both amplitude and phase information.

Example traces of the FROG measurement along with the retrieved pulse shape and phase in the time and frequency domains are given in Fig. 2.

In general, the traces measured by the FROG have large fluctuations. Figure 2 shows cases with single (a) and multiple (b) intensity spikes. The asymmetry in the frequency axis in the trace is an indication of overall energy chirp. While the phases for each spike are very complicated, there are clearly phase discontinuities at the edge of some spikes.

To interpret the observation in Fig. 2, we recall that the temporal characteristics of a SASE pulse, due to the noisy startup, are those of chaotic light. Under the one-dimensional, cold-beam approximation with the electron energy chirp considered, the electric field in the exponential growth regime is a sum of N_e wave packets [12-15]:

$$E(t,z) = E_o(z)\sum_{j=i}^{N_g} \exp\left[i[\omega_j + \Phi''_\gamma(t-t_j-\frac{z}{v_p})](t-t_j-\frac{z}{c}) \right] \quad (1)$$

$$\times \exp\left[-\frac{1}{4\sigma_t^2}(t-t_j-\frac{z}{v_g})^2(1-\frac{i}{\sqrt{3}}) \right],$$

where N_e is the total number of electrons in the bunch, $\omega_j = \omega_0 + 2\Phi''_\gamma(t_j-t_0)$, $v_p = c/(1+\lambda_0/\lambda_u)$, $\Phi''_\gamma = \omega_0 c \sigma_\delta/\sigma_z$ with ω_0 being the instantaneous resonant frequency at t_0, $E_0(z)$ contains the exponential growth factor, t_j is the arrival time of the jth electron, v_g is the group velocity of each wave packet with an rms coherent length $\sigma \approx (N_u/\rho)^{1/2}/2\omega_r$, N_u is the number of undulator periods, and ρ is the FEL scaling parameter [2]. Clearly, an intrinsic chirp exists within a coherent spike as indicated by the quadratic phase term of $(t-t_i-z/v_g)^2/4\sqrt{3}\,\sigma_t^2$ in Eq. (1), and an overall frequency chirp exists from spike to spike through Φ''_γ. Collecting all coefficients of quadratic terms in Eq. (1) and taking into account the dispersion in the collecting optics, the chirp observed by the FROG is

$$\phi'' = \frac{d^2\phi}{dt^2} = -2\,\mathrm{Im}(\Gamma) = 2\frac{\Omega\Theta + \Phi''_m}{\Omega^2 + \Phi''^2_m}, \quad (2)$$

where $\Omega = 4\sigma_t^2 + \Phi''_m\Theta$, $\Theta = 1/3^{1/2} + 4\,\sigma_t^2\,\Phi''_\gamma$, and Φ''_m is the dispersion in the collecting optics of 1.9-cm fused silica.

The experimentally measured chirp $|\phi''|$ for both data sets are given in Fig. 3 (a) and (b) as a function of the coherence length (approximated as the spike length) for
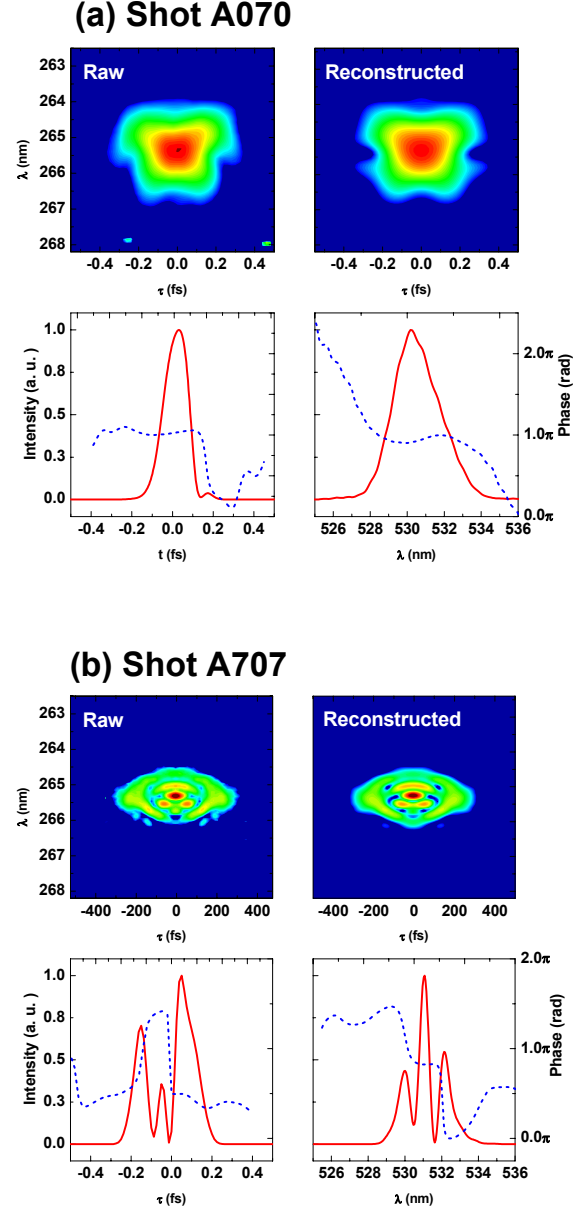

Figure 2: Two sample FROG traces with retrievals, showing the raw and reconstructed traces, as well as the intensity (solid lines) and phase (dashed lines) in the time and frequency domains.

individual spikes. Due to the intrinsic jitter and complicated behavior of each spike, the data are rather scattered. Even so, one can clearly identify a sharp dip at around σ_t=75 and 50 fs for data sets A and B, respectively, that corresponds to $\Theta \approx 0$ in Eq. (2). By slightly adjusting the electron beam energy chirp in Eq. (2), we are able to fit the position of the dips at -28/m and -75/m for data sets A and B, respectively (see curves in Fig. 2). Simulation shows that, the chirp can be due to the uncompensated chirp from the bunch compressor, as well
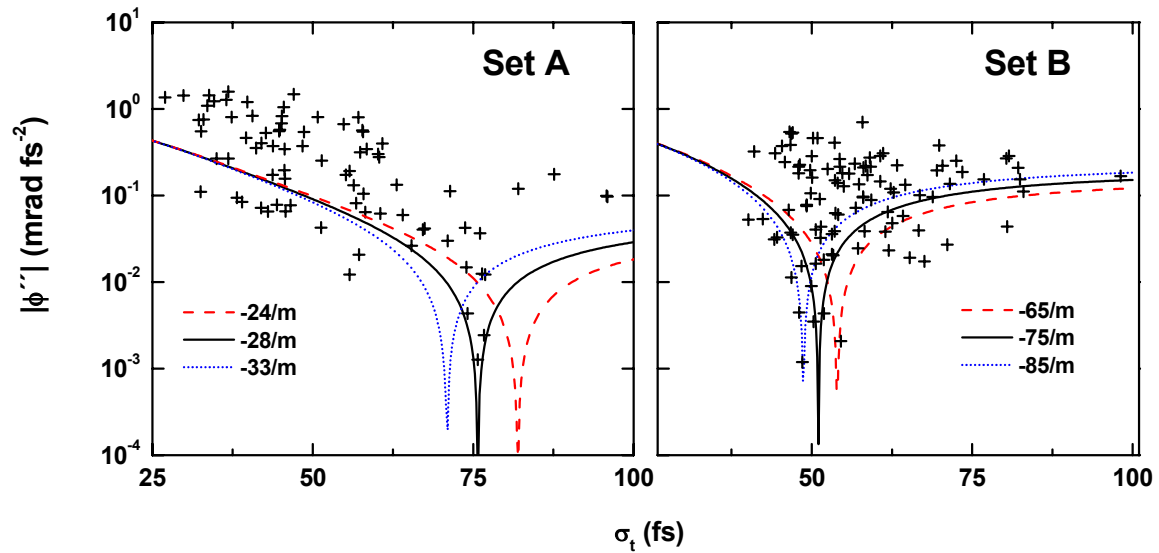
Figure 3: The experimentally measured FEL pulse chirp as a function of the coherence length for experiments A and B. The symbols are the experimental data and the curves are fittings using Eq. (2) with different electron beam chirps.

as the effect of the longitudinal wake field, if not intentionally imposed.

The results in Fig. 3 unambiguously reveal the positive intrinsic SASE chirp. They also verify that the electron beam energy chirp directly maps into the FEL output, a key process for compressing and slicing the pulse from future X-ray FELs. Figure 3 also serves as an independent measurement of the electron bunch energy chirp.

The FROG traces also provide rich information on the statistics of the SASE output, especially the temporal information on these pulses. As the FROG traces provide the information in the frequency domain simultaneously, a correlation analysis between the time and the frequency domain is now possible. A more detailed analysis of the statistics is underway.

SUMMARY

In conclusion, we observed a positive intrinsic chirp in the SASE FEL spikes, and we confirmed that the energy chirp in the electron bunch does map to the SASE output. These observations have very important applications for future X-ray FEL sources in pulse engineering and manipulation.

The authors are grateful for help by O. Markarov and R. Dejus for performing the gain length measurement and processing the data. We also thank L. Teng for insightful discussions.

REFERENCES

[1] A. M. Kondratenko, E. L. Saldin, Sov. Phys. Dokl. **24** (12), 986 (1979).

[2] R. Bonifacio, C. Pellegrini, L. M. Narducci, Opt. Commun. **50**, 373 (1984).

[3] M. Cornacchia et al., "Linac Coherent Light Source (LCLS) Design Study Report," Report SLAC-R-521 (Stanford Linear Accelerator Center, Stanford, CA), revised 1998.

[4] R. Brinkmann, G. Materlik, J. Rossbach, A. Wagner, Eds., "Conceptual Design of a 500 GeV e^+e Linear Collider with Integrated X-Ray Laser Facility," DESY Report DESY97-048 (Deutsches Elektronen-Synchrotron, Hamburg), 1997.

[5] S. V. Milton et al., Science **292**, 1953 (2001).

[6] V. Ayvazyan et al., Phys. Rev. Lett. **88**, 104802-1 (2002).

[7] A. Tremaine et al., Phys. Rev. Lett. **88**, 204801-1 (2002).

[8] S. G. Biedron et al., Nucl. Instrum. Methods Phys. Res. A **483**, 94 (2002).

[9] R. Trebino et al., Rev. Sci. Instrum. **68**, 3277 (1997).

[10] Y. Li et al., Phys. Rev. Lett. **89**, 234801 (2002).

[11] E. Gluskin et al., Nucl. Instrum. Methods Phys. Res. A **429**, 358 (1999).

[12] R. Bonifacio et al., Phys. Rev. Lett. 74, **70** (1994).

[13] K.-J. Kim, "Towards X-ray free electron lasers," AIP Conference Proc. 413, R. Bonifacio and W. A. Barletta, Eds. (American Insitute of Physics, New York), p. 3 (1997).

[14] C. B. Schroeder et al., Nucl. Instrum. Methods Phys. Res. A **483**, 89 (2002).

[15] S. Krinsky and Z. Huang, Phys. Rev. ST-AB, in press.